Modelling the fluid flow inside a refrigerated trailer loaded with prok carcasses

Mouna Merai, Onrawee Laguerre, Steven Duret, D. Flick

Manuscript ID: 178
DOI: 10.18462/iir.icr.2019.0178

Modelling the fluid flow inside a refrigerated trailer loaded with pork carcasses

Mouna MERAI[(a)], Steven DURET[(a)], Jean MOUREH[(a)], Onrawee LAGUERRE[(a)], Denis FLICK[(b)]

[(a)] Irstea, Refrigeration Process Engineering RU
Antony, 92761, France, steven.duret@irstea.fr

[(b)] AgroParisTech, Inra, Université Paris-Saclay, Food Process Engineering JRU
Massy, 91300, France, denis.flick@agroparistech.fr

ABSTRACT

When pork carcasses are transported in a refrigerated trailer, all of them should be correctly ventilated. CFD simulations were performed to assess the homogeneity of air circulation around the carcasses. From an Xray scanner of a carcass, a simplified geometry was deduced. The air volume inside a semitrailer containing 430 pork half-carcasses was then meshed (21.10^6 cells). The Reynolds Averaged Navier Stokes equations were solved with the k-ε turbulence model. The flow pattern is very complex: air is blown at high velocity on the top of the container front, forming a wall jet. There is an air entrainment by this jet whose section increases whereas its velocity decreases. Part of the blown air flows throughout the 'porous' zone constituted by the carcasses while another part reaches the gap between the carcasses and the doors at the rear of the container. Finally air flows back toward the outlet. Zones of low velocity between half-carcasses were identified.

Keywords: Aeraulics, Carcass, Computational Fluid Dynamics, Refrigerated vehicle

1. INTRODUCTION

When pork carcasses are transported in a refrigerated trailer, all of them should be correctly ventilated. But in fact, it has be shown both by experimentation and computational fluid dynamics (CFD) that air flow can be very heterogeneous in refrigerated trailers. Up to now, the studies concerned empty trailers (Moureh and Flick 2005), trailers loaded with impermeable or porous pallets (Tapsoba et al. 2007, Moureh et al. 2009) or a single carcass (Pham et al. 2009, Kuffi et al. 2016).

The present study concerns the case of a long trailer (13.3 m) loaded with 430 pork half-carcasses. The air inlet and outlet are both located at the front of the container, this generally implies a better ventilation in the front part than in the rear part. The air is blown at high velocity (11 m/s) near the ceiling of the container front, forming a turbulent wall jet. The particularity of this configuration in comparison with previous studies is the very complex geometry of the load. A numerical approach is here presented.

Many CFD studies of air flow in refrigeration equipment use the Reynolds Averaged Navier Stokes (RANS) approach. The objective is to predict the time-averaged mean velocity ($\vec{v}$). Most often the Reynolds stresses, due to the velocity fluctuations ($\vec{v}'$) are expressed with the Boussinseq approximation by introducing the turbulent viscosity (ν_t). This way, the eddies are not directly solved but only characterized by their turbulent kinetic energy (k). Following Kolmogorov's point of view, mechanical energy of the mean flow is transformed into turbulent kinetic energy (because of the mean velocity gradients) and the energy of the smallest eddies is transformed into heat (molecular agitation) with a specific dissipation rate (ε). For complex geometries, an algebraic estimation of the turbulent viscosity cannot be used; the most popular approach relates ν_t to k and

ε (taking into account indirectly of the turbulence length scale l_t). Different versions are available which differ by some energy redistribution terms and near wall treatment (standard k-ε. realizable k-ε, k-ε RNG, k-ω SST). Near wall treatment is especially important if heat transfer has to be predicted. Sometimes the Boussinesq approximation cannot be applied because eddies are highly anisotropic and more sophisticated model (e.g. RSM) have to be used (Defraeye et al. 2013).

Near the walls, $\vec{v}$ varies very rapidly in a nonlinear way, so that a very fine mesh should be employed near the walls. But this becomes very expensive in term of memory and computing time. Therefore, assuming that the flow is almost parallel to the wall in the first cell near a wall, the boundary layer theory can be employed to estimate the wall shear stress. In the software the employed near wall relations are called 'wall functions'.

The present study aims to predict the homogeneity of the fluid flow around the carcasses. No precise velocity field or estimation of the heat transfer intensity is expected; therefore the standard k-ε model (with wall functions) was used.

2. GEOMETRY AND MESH

Fig.1 presents the dimensions of the trailer and of the zone occupied by the carcasses.

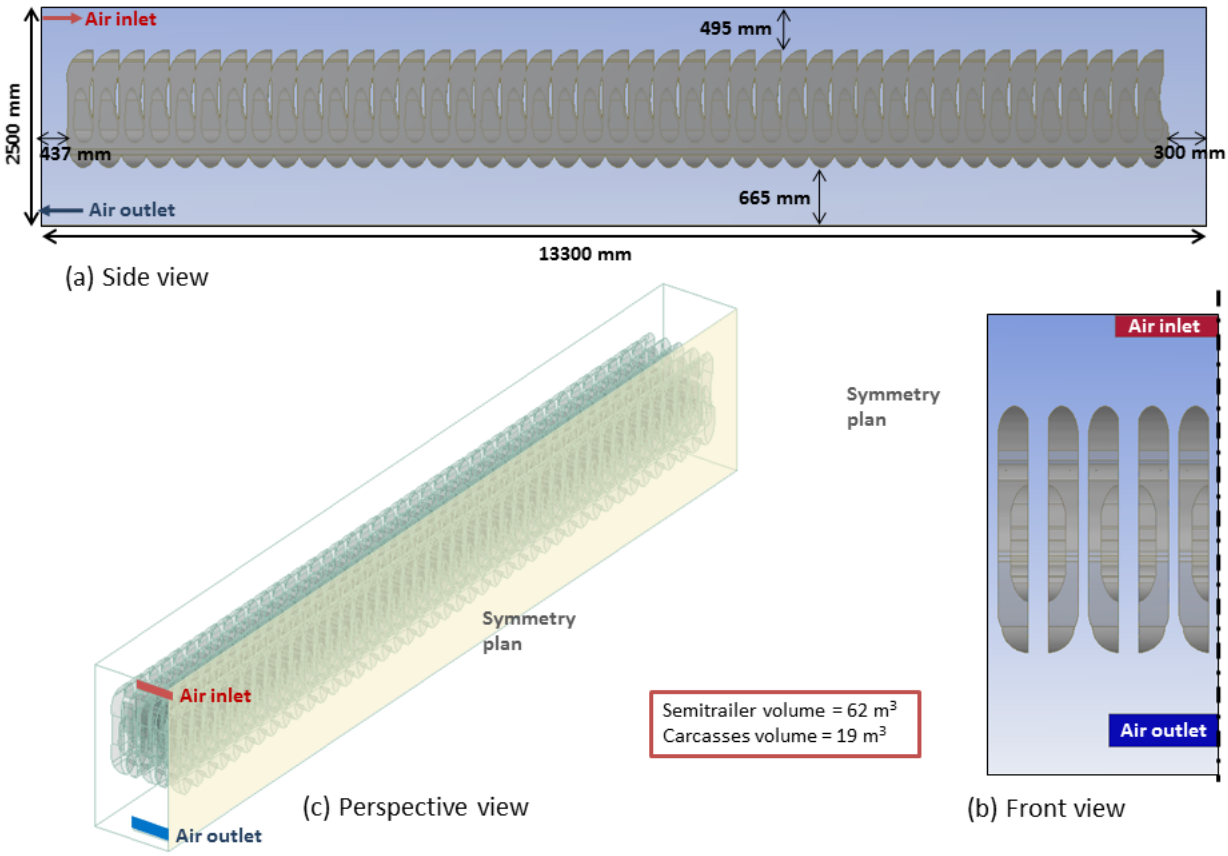

Figure 1: Dimensions of the trailer (real scale)

From an Xray scanner of a carcass, a simplified geometry was deduced as shown on Fig. 2.

The simplified geometry was developed in order to have the same volume ensuring the same porosity of the zone occupied by the carcasses. The horizontal section at a given height is also about the same for the real carcass and the simplified geometry, ensuring almost the same convergent or divergent flow in the vertical direction.

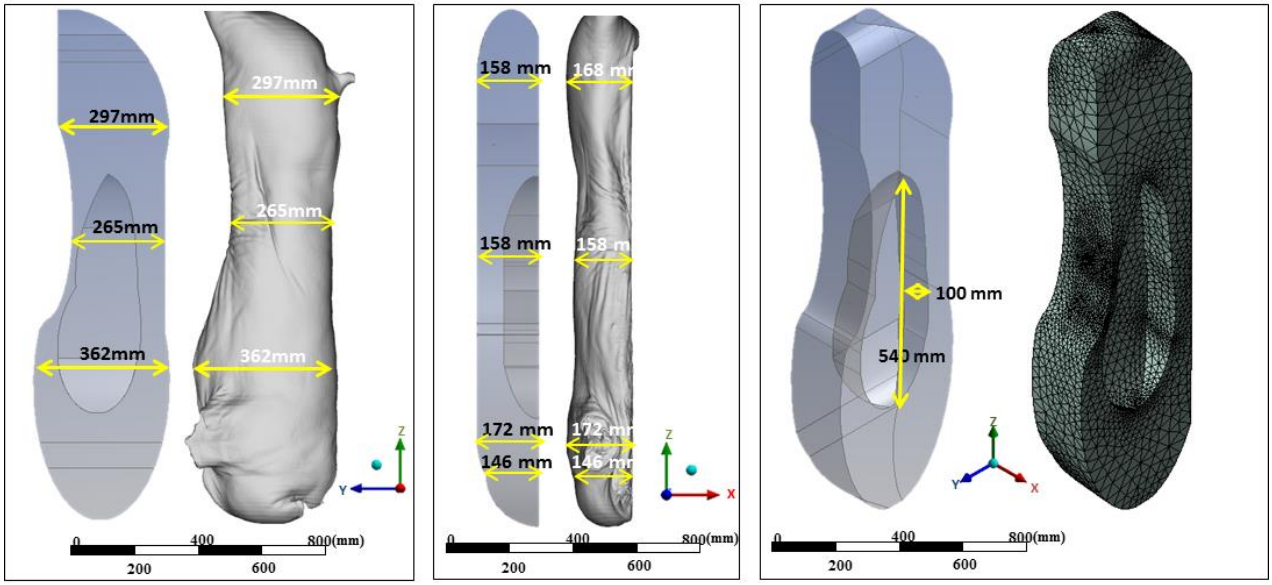

Figure 2: Simplified geometry of the carcasses

The air volume inside a semitrailer containing 430 pork half-carcasses was then meshed using 21 009 342 cells (Fig. 3). Near the top wall, the mesh is prismatic in order to better take into account the wall jet development.

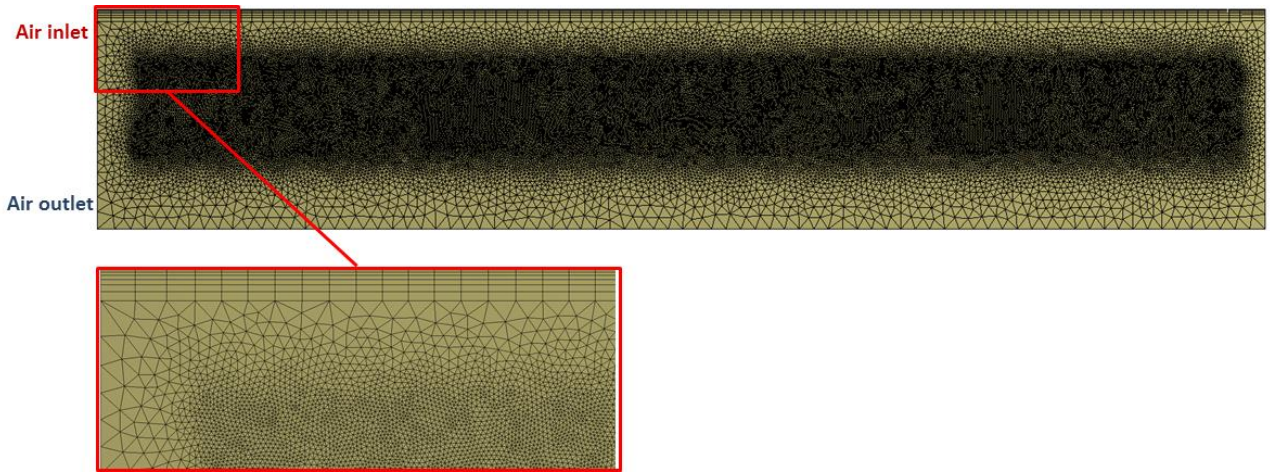

Figure 3 View of the mesh

3. MAIN HYPOTHESES AND BOUNDARY CONDITIONS

The fluid was assumed incompressible and isothermal. Properties of air at 4°C were used.

The steady state Reynolds Averaged Navier Stokes (RANS) equations with the standard k-ε model of turbulence and the standard (logarithmic) wall function (smooth walls) were solved using the finite volume method (Fluent).

The inlet conditions are:
- section 1.100 m x 0.16 m (hydraulic diameter: 0.28 m)
- normal mean velocity: 11 m/s (Reynolds number: $2.2\ 10^5$)
- turbulence intensity: 10 %
- turbulence length : 7% of hydraulic diameter

At outlet, uniform pressure was imposed (without viscous stress).

The simulation converged after 3500 iterations which needed 48 hours of computation on a 12 cores computer with 130 Go RAM.

4. RESULTS AND DISCUSION

Fig. 4 present some computed stream lines inside the loaded trailer (the carcasses are not represented in this figure but where taken into account in the simulation). This highlights the complexity of the 3D flow pattern. Globally air blown near the ceiling forms a wall jet. Its section increases whereas its velocity decreases (1). It adheres to the top wall (by Coanda effect) nearly up to the rear of the trailer. Part of the blown air flows throughout the ‘porous’ zone constituted by the carcasses while another part reaches the gap between the carcasses and the doors at the rear of the container (2). Finally air flows back toward the outlet near the bottom (3). There is an air entrainment by the jet which explains an upward flow on the front of the trailer (4).

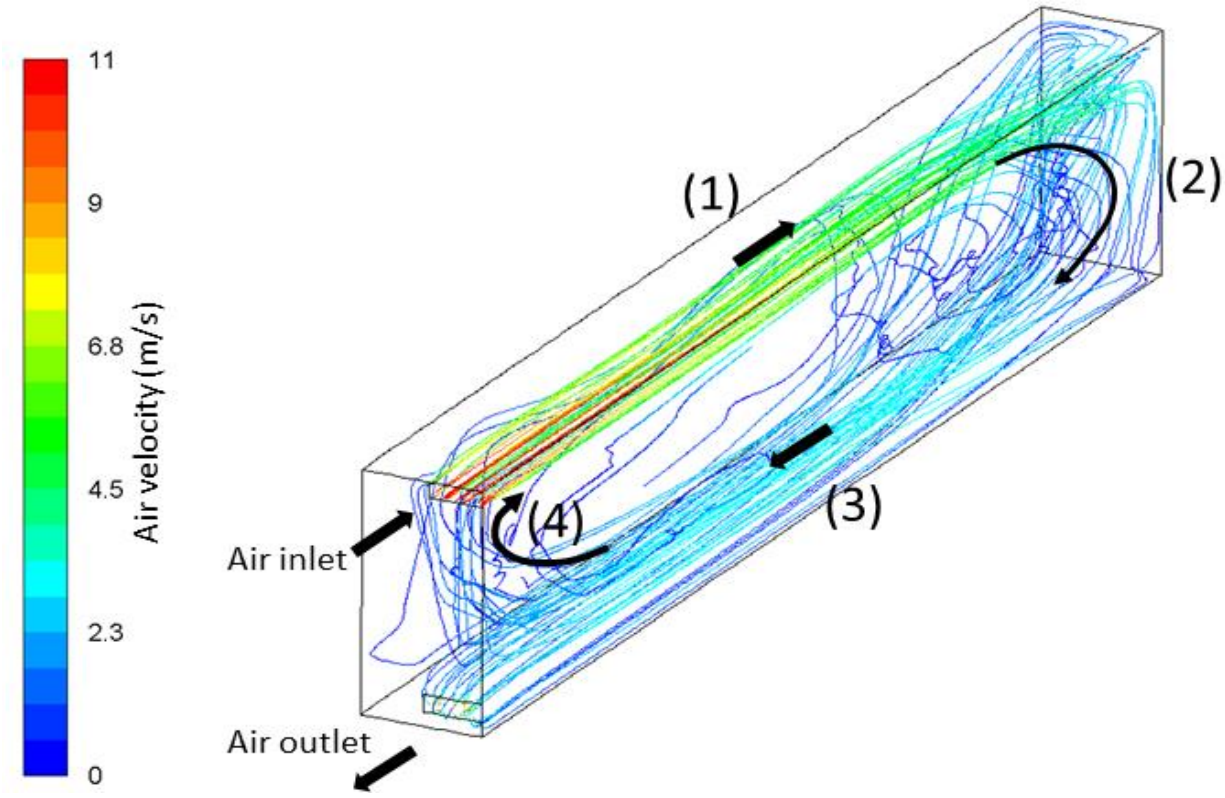

Figure 4 : Stream lines issued from the inlet section

Fig. 5a presents the computed velocity magnitude in the symmetry plan. This velocity field can be compared outside the zone of carcasses with the experimental one (Fig. 4b) which was obtained on a reduced scale trailer loaded with reduced scale carcasses made of polyurethane foam (Merai et al. 2018) by 2D Laser Doppler Velocimetry (LDV).

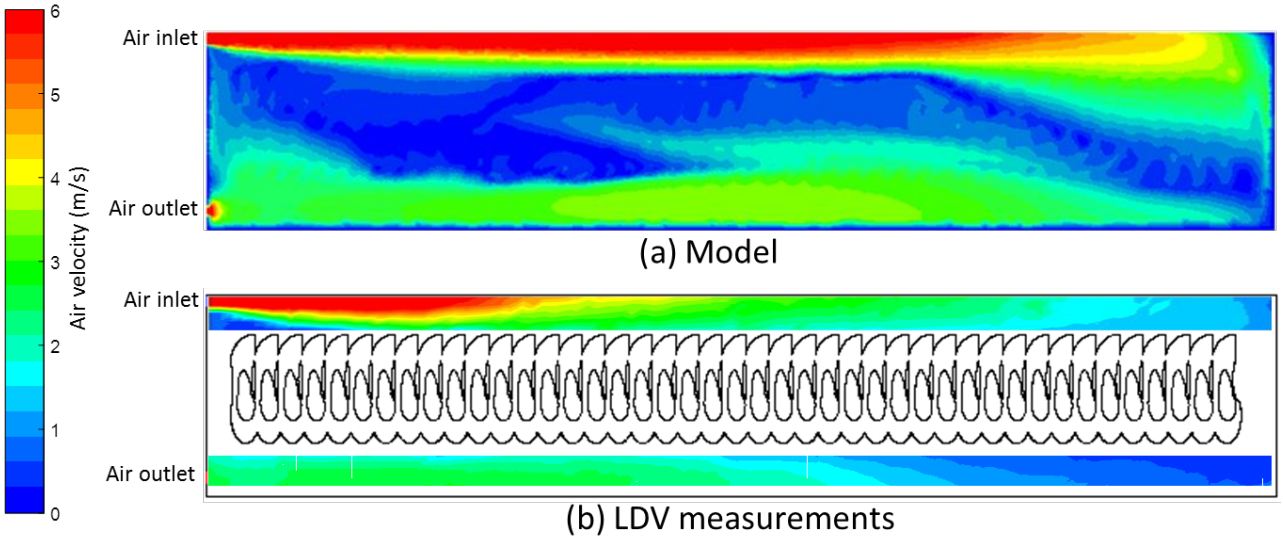

Figure 5: velocity magnitude in the symmetry plan (red color represents velocities ranging from 6m/s to 11 m/s which is the value at inlet)

Fig. 6 compares the evolution along the jet axis (longitudinal axis passing by the center of the inlet section) of the numerical and experimental axial velocities.

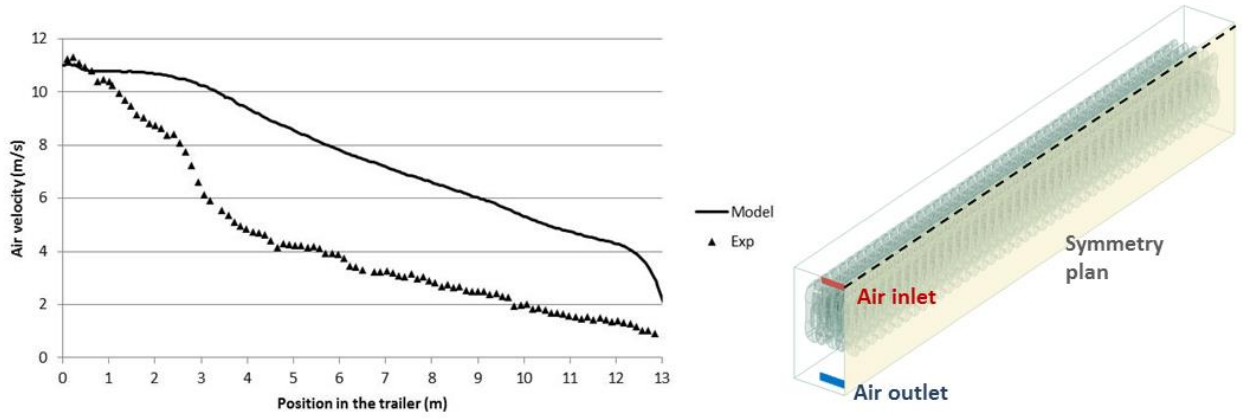

Figure 6 : Velocity along the jet axis

The main difference is that the predicted velocity decreases less rapidly along the jet axis than the measured one. This can be explained by several reasons. The simulated geometry does not take into account the presence of the hooks and the extremity of the feet. Also the heights at which the carcasses are hanged is not exactly the same in the experiment (and in real configuration) to the contrary of simulation. All these aspects could contribute to produce turbulence and increase the jet diffusion in the lateral and vertical directions. The k-ε model is also known to predict incorrectly flows with adverse pressure gradients. This explained that for of an empty trailer, the k-ε was unable to predict the experimentally observed separation of the jet from the wall (Moureh and Flick 2005) whereas the RSM model, which better takes into account of turbulence anisotropy, predicted it well. More realistic geometry and more advanced turbulence models will be tested in future work.

Nevertheless, even taking in mind the limitations of the present numerical results, the interest of the CFD approach is that, contrarily to the experimental approach, it is possible to estimate the air flow around the carcasses.

Fig. 7 presents the velocity magnitude at different position between the half carcasses. Some zones of low velocity between half carcasses can be identified.

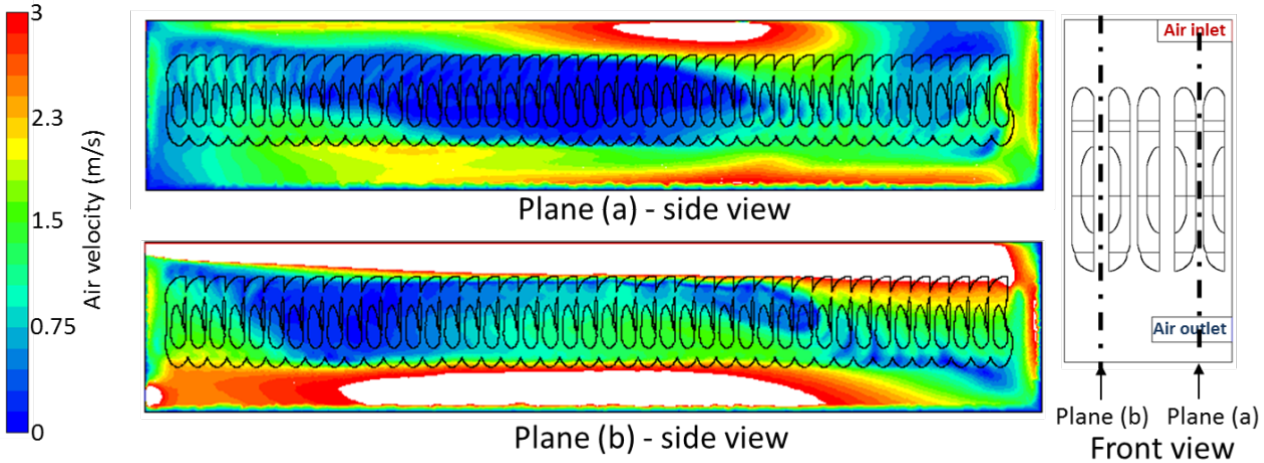

Figure 7 : Velocity magnitude between half carcasses

In plane (a) notably, a nearly stagnant zone at mid length of the trailer was predicted because the simulated jet wall continued flowing along the top wall until the rear of the trailer. In fact, according to the experimental velocity evolution on the jet axis, is seems that less air reaches the trailer rear and more air flows downward through the carcasses.

Fig. 8 present the vertical velocity component at mid height of the trailer. One could imagine that the carcasses form a porous medium of relative high pressure drop and that since the air is blown on the top, a relative homogenous downward airflow would occur throughout the carcass zone. But in fact, near the trailer rear the flow is indeed downward but near the front, the entrainment effect of the wall jet induces a suction effect and air flows upward throughout the carcasses in the front zone. In the intermediate region, there is sometimes neither downward and neither upward flow leading to low velocity zones.

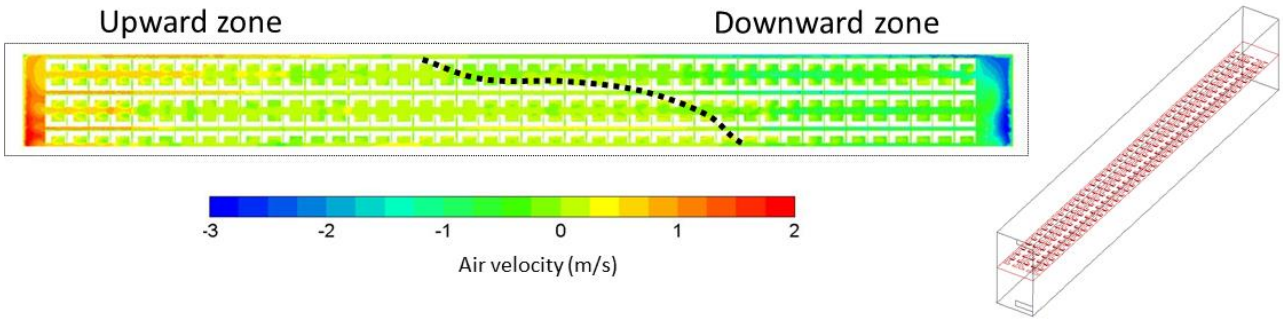

Figure 8: Vertical velocity (positive upward) at mid height of the trailer

In the zones of low velocity, the refrigeration will be of low intensity. Thus, if the carcasses are loaded while there are still warm at core (e.g. 15°C at core and 7°C at surface), they could take a long time to reach everywhere the recommended temperature (<7°C). Even the surface temperature could slightly increase. This can be problematic for sanitary risk (pathogenic microorganism growth). In fact, the smallest velocities are observed in the loan region of the carcasses (at mid height of the carcasses). Since the loan thickness is small (compared to the jam for example) the loan is generally rapidly cooled down in the cold room of the slaughterhouse. So, microbial risk should be limited for the loan part. In opposite, the jam core is often the warmest part at the exit of the slaughterhouse but the velocity is rather high all along the trailer at the top of the carcasses (jam part). The shoulder regions are also quite well ventilated.

5. CONCLUSIONS

Numerical simulations were performed to determine the air flow distribution in a refrigerated trailer loaded with pork half carcasses using the standard k-ε model. In the studied configuration, some low velocity zones were located in the loan region of the carcasses but this should not be problematic for sanitary risk.

These numerical results are specific of the trailer geometry (inlet and outlet section and location, number of rails) and of the load (here 215 pork carcasses about 75 kg each). The numerical approach could be used to see the influence of the trailer configuration, including the effect of air ducts, and of load (lower or higher number of carcasses) on the airflow distribution.

Nevertheless, the numerical model should be improved, because it overestimates the flow rate which reaches the rear of the trailer. In further work, a more realistic geometry and more sophisticated turbulence model (e.g. RSM or k-ω SST) will be tested and the simulation will also integrate unsteady heat transfer.

ACKNOWLEDGEMENTS

This research work was carried out within the framework of a DIM ASTREA grant by the Regional Council of Ile-de-France (France).

REFERENCES

Defraeye T., Verboven.P. Nicolai B. (2013) CFD Modeling of flow and scalar exchange of spherical food products; turbulence and boundary layer modelling. Journal of food engineering 114, 495-504.

Kuffi K.D., Defraeye T., Nicolai B., De Smet S., Geeraerd A., Verboven P. (2016) CFD modelling of industrial cooling of large beed carcasses. International Journal of Refrigeration 69, 324-339.

Merai M., Flick D., Guiller L., Duret S., Laguerre O. (2018) Experimental characterization of airflow inside a refrigerated trailer loaded with carcasses. International Journal of Refrigeration, 88, 334-346.

Moureh J. Flick D. (2005) Airflow characteristics within slot ventilated enclosures. International journal of heat and fluid flow, 26, 12-24.

Moureh J., Tapsoba M.S., Derens E., Flick D (2009). Air velocity characteristics within vented pallets loaded in a refrigerated vehicle with and without air ducts. International Journal of Refrigeration 32, 220-234

Pham Q.T., Trujillo F.J,. McPhail N. (2009) Finite element model for beef chilling using CFD-generated heat transfer coefficients. International Journal of Refrigeration 32, 102-113.

Tapsoba M.S., Moureh J., Flick D (2007). Airflow patterns in a slot-ventilated enclosure partially loaded with empty slotted boxes. International Journal of Heat and Fluid Flow 28, 963-977.